

Oxygen Transfer Performances of Unbaffled Bio_Reactors with Various Aspect Ratios

Francesca Scargiali*, Antonio Busciglio, Franco Grisafi, Giorgio Micale, Alessandro Tamburini, Alberto Brucato

Dipartimento di Ingegneria Chimica, Gestionale, Informatica e Meccanica, Università degli Studi di Palermo - Viale delle Scienze, 90128 Palermo
francesca.scargiali@unipa.it

Cultivation of microorganisms, plants or animal cells requires liquid agitation in order to ensure oxygen and nutrient transfer and to maintain cell suspension. Many studies on animal cell damage due to mechanical agitation and sparging aeration have shown that mechanical damage of freely suspended animal cells is in most cases associated with bursting bubbles at the air–liquid interface (Barrett *et al.*, 2010).

Gas bubbles are usually generated by direct air sparging aimed at supplying oxygen to the culture medium. Mechanical agitation may also introduce gas bubbles in the culture medium via vortexing entrainment from the free surface.

In this work oxygen transfer performance of an unbaffled stirred bioreactor, with various aspect ratios, is presented in view of its use as a biochemical reactor for animal cell growth. In practice oxygen mass transfer occurs through the (more or less deep) free surface vortex which takes place when agitation is started in unbaffled vessels. If this vortex is not allowed to reach impeller blades, bubble formation and subsequent bursting at the free-surface is avoided.

Experimental results show that this kind of bioreactor can provide sufficient oxygen mass transfer for animal cell growth, so resulting in a viable alternative to the more common sparged reactors. The mass-transfer performance observed with the different aspect ratio configurations is also presented and discussed.

1. Introduction

Despite being poorer mixers than baffled vessels, unbaffled stirred tanks are enjoying a growing interest in the process industry, as they provide significant advantages in a number of applications where the presence of baffles is undesirable for some reason (Tamburini *et al.*, 2013). This is for instance the case of crystallizers, where the presence of baffles may promote particle attrition (Hekmat *et al.*, 2007), or in food and pharmaceutical industries, where vessel cleanness is a topic of primary importance (Assirelli *et al.*, 2008), as well as in bioslurry reactors for soil remediation processes, where air presence within the tank may be guaranteed by the central vortex formation instead of an intrinsically more expensive and troublesome insufflation device, due to sparger hole blocking by particles. (Tamburini *et al.*, 2012). As concerns bioreactor applications, when shear sensitive cells are involved, mechanical agitation and especially sparging aeration (and associated bubble bursting) can cause cell death (Chisti, 2000). In unbaffled vessels, at low agitation speeds, the required oxygen mass transfer may well take place through the free surface deep vortex which takes place when agitation is started (Scargiali *et al.* 2012a). This feature clearly makes unbaffled vessels potentially advantageous for shear sensitive cultures (e.g. animal cell or filamentous mycelia cultures) as well as for many foaming gas-liquid systems, provided that process rates, and relevant gas consumption needs, are compatible with the relatively small gas transfer rates achievable (Scargiali *et al.*, 2014).

In this work oxygen transfer performance of unbaffled stirred bioreactors with various aspect ratios is presented, in view of their use as biochemical reactors for animal cell growth.

2. Experimental

The investigated reactor is depicted in Fig.1a. It consisted of a flat bottomed cylindrical tank with an internal diameter of 280 mm and an height of 1450 mm. A 0.095 m diameter six-flat-blade hub-mounted turbine (Fig. 1b) was mounted on the 17 mm dia. shaft, at a clearance $C=20$ mm.

Stirrer shaft was driven by a 1200W DC motor (Mavilor MSS-12), equipped with tacho and speed control unit (Infranor SMVEN 1510) so that rotational speed was maintained constant, within 0.1%. Rotational speeds ranged from 100 to 1100 rpm in order to explore different fluid-dynamics regimes occurring inside the unbaffled stirred reactor. The vessel was filled with deionized water up to an height H (under no agitation conditions) of 280 mm ($H=T$), 560 mm ($H=2T$) and 840 mm ($H=3T$) respectively.

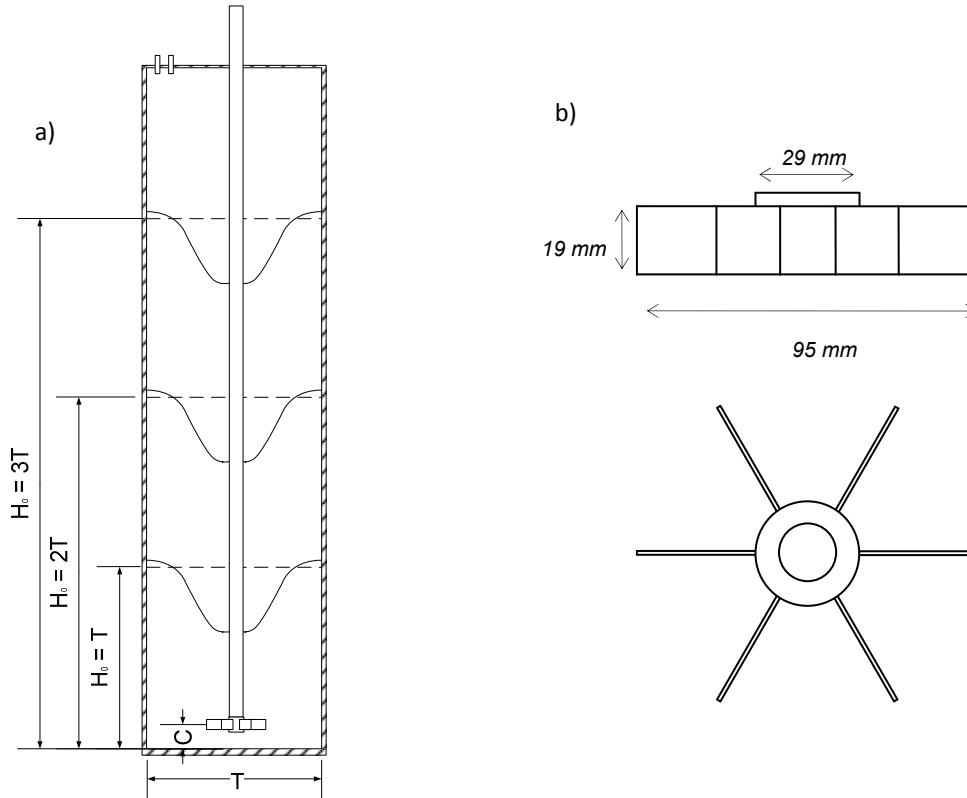


Fig. 1: a) Schematic diagram of the experimental apparatus; b) radial turbine

Power consumption measurements were carried out by monitoring the temperature rise due to the agitation power input (Scargiali *et al.*, 2012b). All temperature dynamics showed a remarkably constant slope. For simplicity, in the computation of power dissipation the heat capacity of vessel walls, shaft and impellers were neglected in front of that of the water mass. Also, heat exchange through vessel walls was neglected, on the basis of the very small temperature differences between water and ambient air (always smaller than 0,5 °C, as each run was started from equilibrium conditions). This allowed to directly converting the observed temperature rise speed (e.g. $3.07 \cdot 10^{-4}$ °C/s at 850 rpm) into the relevant specific dissipation rate (1555 W/m^3 of liquid phase). The total agitation power was finally estimated by multiplying specific power dissipation by the system water volume (e.g. 0.0344 m^3 for $H=2T$).

The volumetric mass transfer coefficient, $k_L a$, was assessed via unsteady-state experiments by means of the simplified dynamic pressure method (SDPM) (Scargiali *et al.*, 2010a), a technique that was found to be particularly suitable for $k_L a$ assessment in culture media and fermentation broths. In this method the driving force for oxygen absorption is obtained by a sudden change of vessel pressure, with no need for sudden gas phase composition changes. For a perfectly mixed system, if $k_L a$ and the interfacial gas concentrations are identical for all bubbles at any time, equation (1) is obtained:

$$\ln\left(\frac{C_L^* - C_L}{C_L^* - C_L^0}\right) = -k_L a (t - t_0) \quad (1)$$

where C_{L0} , C_L and C_L^* are the initial (time zero), instantaneous (at time t) and interfacial (viz equilibrium) oxygen concentration in the liquid phase, respectively. Eqn.1 shows that, if the above hypothesis are reasonably abode by, plots of $\ln(C_L^* - C_L)$ versus t should result into straight lines with a slope equal to $(-k_L a)$. This is not rigorously true, due to the contemporaneous nitrogen transport effects, but these can be accounted for by applying a correction factor to the measured slopes, as described by Scargiali and co-workers (Scargiali et al., 2010b). This correction however becomes significant only for quite large $k_L a$ values, and in practice was never needed in the present work. Notably the technique is unaffected by the extent of the oxygen probe response time, as long as it remains smaller than the reverse of the $k_L a$ value measured (see Scargiali et al., 2010a for a thorough discussion on this topic) a condition which was amply met by all of the present data.

An inexpensive Venturi vacuum pump fed by compressed air (Vaccon HVP 100) was used to evacuate the vessel down to an inside initial pressure of about 0.1 bar. Oxygen concentration in the liquid phase was measured by an electrode sensor (WTW CellOx 325) and control unit (WTW Oxi 340i). The output of the oxygen measurement unit was recorded by a data acquisition system and processed to yield the relevant value of the mass transfer coefficient $k_L a$ (Scargiali et al., 2013a).

In all runs temperature inside the reactor was between 20 and 21 °C. This was obtained by adjusting the initial temperature and exploiting the circumstance that the temperature increase during each single run was always less than 0.2 °C.

3. Results and discussion

3.1 Fluid dynamic regimes

As already observed in “standard” unbaffled stirred vessels (Busciglio et al., 2013) when the stirrer is operated at the lowest rotational speeds no gas dispersion occurs inside the reactor and a vortex appears on the free surface with a depth increasing as rotational speed increases (*sub-critical regime*). At high velocities vortex bottom overcomes the impeller leading to bubble injection in the liquid phase, that are then radially entrained by the impeller stream towards vessel wall. Afterwards, while moving upwards under the effect of gravity, they undergo a centripetal acceleration towards the central vortex, due to their smaller density with respect to the liquid phase. These events result in practice in the formation of a gas-liquid dispersion (*super-critical regime*) in a significant portion of vessel volume.

Notably, at the impeller speed at which vortex bottom just reaches the impeller plane no bubbles are still ingested in the liquid phase: this implies that in order to reach the *super-critical regime*, characterized by significant gas ingestion, agitation speed needs to be further increased.

3.2 Power consumption

The total power dissipations experimentally obtained at the various agitation speeds and vessel configurations were translated into the relevant power number (N_p) values, defined as

$$N_p = \frac{P}{\rho_L N^3 D^5} \quad (2)$$

where P is agitation power, ρ_L is liquid density, N is agitation speed (s^{-1}) and D is impeller diameter. Power Number results are reported in Figure 2 for the three cases investigated: H=T; H=2T and H=3T. As it can be observed in all investigated configurations power number *versus* Reynolds number curves show a slightly-decreasing behavior as long as the free surface vortex does not reaches the impeller (non-aerated regime, $N < N_{crit}$), while a steep decreasing trend is observed after vortex reaches the impeller plane and air bubbles begin to be dispersed inside the reactor ($N > N_{crit}$), much in the same way as previously observed by Scargiali et al (2013b) in Rushton turbine stirred unbaffled vessels. This may depend on the formation of gas pockets (called cavities) behind stirrer blades, as observed in baffled sparged gas-liquid reactors,

as well as on the progressive uncovering of part of the blades, due to the growing vortex diameter at impeller height.

It may be worth noting that at the same Reynolds number (same agitation speed) N_p increases as liquid height H (viz liquid volume) increases, as expected in view of the larger surface attrition against reactor wall. One might wonder whether a simple proportionality exists between the two, i.e. between N_p and H/T (proportional to side wall), or between N_p and total wet "holding" surface including tank bottom (proportional to $(1+4H/T)$). As both of these N_p corrections resulted in an overcorrection of N_p values, corrections based on the assumption that, due to the much closer vicinity to the stirrer, friction on tank bottom was significantly larger than that on side wall, were attempted, eventually resulting in a normalizing factor simply given by $(1+H/T)$. The resulting graph is reported in Fig.2b where it can be observed that the normalization adopted is very effective under subcritical conditions, while is less effective above Re_{crit} , especially for the lowest H/T ratio. As for the applications addressed in this work (animal cell culture) only subcritical conditions are of interest, the above normalizing factor devised is endorsed and use of Fig. 2b is recommended for evaluating power consumption in vessels with aspect ratios intermediate between those here investigated and operated in sub-critical conditions.

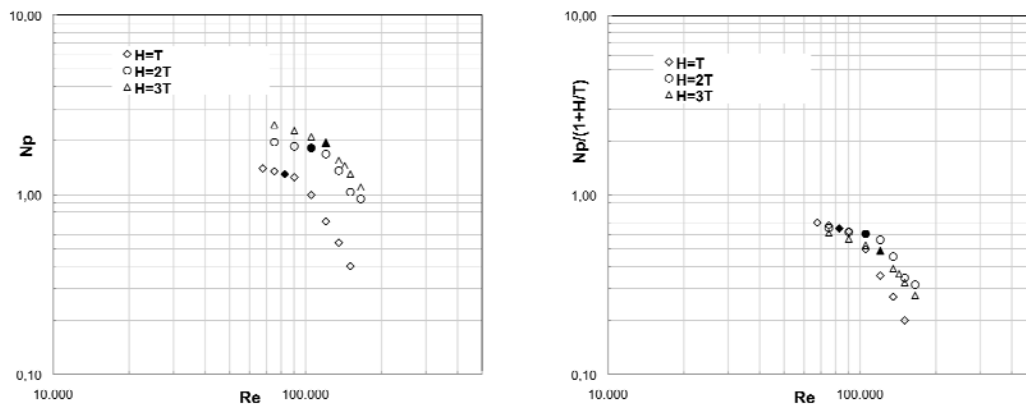


Fig.2: Experimental Power Number N_p (left) and relevant normalized Power Number $N_p/(1+H/T)$ (right) versus Reynolds number Re for the three reactor configurations investigated; Solid symbols mark the critical Reynolds number at which the free surface vortex reaches the impeller (Re_{crit}) and relevant Power Numbers $N_{p,crit}$.

3.3 Gas-liquid mass transfer

The $k_L a$ values obtained by means of the SDPM technique (Scargiali *et al.*, 2010a) in the three investigated configurations are reported in Figure 3 as a function of rotational speed. In the same figure black symbols mark critical rotational speed (N_{crit}) and relevant mass transfer coefficients ($k_L a_{crit}$) at which significant gas dispersion starts. For all three liquid levels the mass transfer coefficient increases as rotational speed is increased, while at the same rotational speed mass transfer coefficient decreases when liquid volume is increased. This phenomenon can be explained observing that, for a given rotational speed N , the free surface vortex depth (hence vortex surface) becomes slightly lower the higher the initial liquid levels H , while liquid volume is proportionally increased, so resulting in a significantly smaller interfacial area per unit volume a . In the mean time turbulence levels are more or less the same resulting in similar values for the mass transfer coefficient k_L , so giving rise to the observed $k_L a$ dependence on H/T .

On the other hand, while increasing H/T , the critical rotational speed N_{crit} increases, due to the lower vortex depth and especially to the larger impeller distance from the liquid free surface. When comparing the critical conditions at increasing H/T , clearly the larger critical rotational speed gives rise to larger values of k_L in conjunction with larger values of the (deeper) critical vortex area, hence somewhat counteracting the liquid volume increase. Notably, this results into practically identical critical $k_L a$ values while varying liquid height, as can be appreciated by observing the solid symbols in Fig. 3.

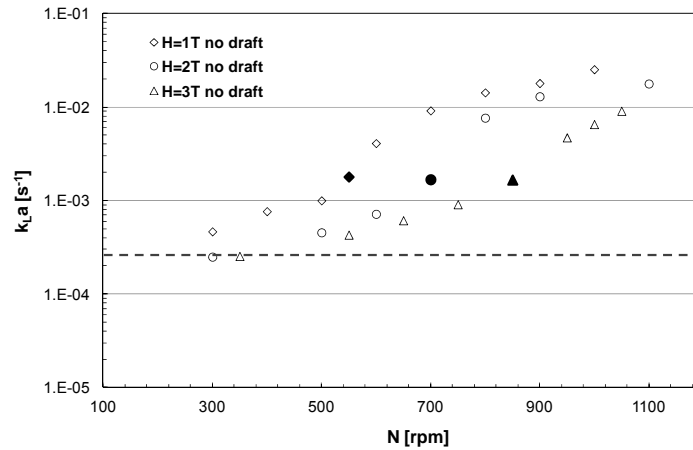


Fig.3 Experimental mass transfer coefficient vs rotational speed for the three reactor configurations investigated. Solid symbols mark the critical rotational speed at which gas dispersion starts (N_{crit}) and relevant mass transfer coefficients. Dashed horizontal line represents minimum k_{La} requirements for animal cell culture, according to Barrett *et al.* (2010).

It is worth noting that in order to avoid gas dispersion inside the reactor, so preserving cells from bubble burst damage, an operating agitation speed smaller than the critical one (N_{crit}) is recommended. In the present system this practically implies a maximum k_{La} value of the order of $1.7 \cdot 10^{-3} \text{ s}^{-1}$ independently of liquid height, as highlighted in Table 1 or by the black symbols in Figure 3. As this value is much higher than the minimum value of about $2.8 \cdot 10^{-4} \text{ s}^{-1}$ required to support animal cell cultures at a typical culture concentrations of about 10^6 cells/ml (Barrett *et al.*, 2010), it can be concluded that the investigated bioreactor, when operated at sufficiently high sub-critical agitation speeds, is fully able to satisfy the Oxygen Transfer Rate demand of current animal cell cultures, independently of the liquid aspect ratio configuration.

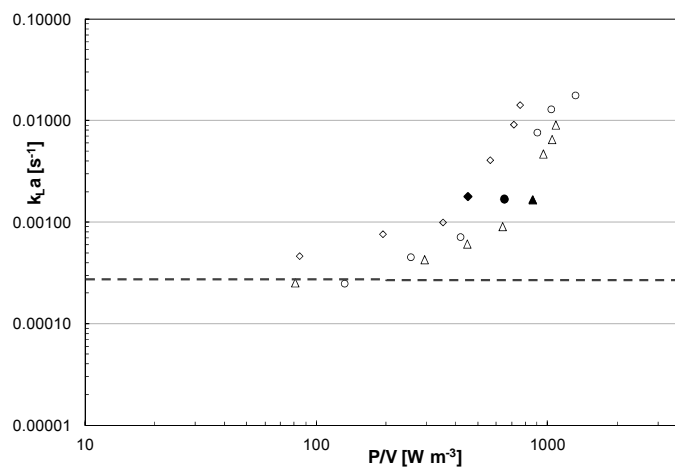


Fig.4 Mass transfer parameter versus specific power demand. Solid symbols mark critical conditions. Legend as in Fig.3.

In order to look at power requirements, in Figure 4 the same data of Figure 3 are reported versus *specific power input*. Results indicate that the higher the H/T the larger the specific power dissipation required to achieve the same k_{La} values. This implies that better energy efficiency is obtained by adopting relatively small H/T ratios.

It is worth noting however that, although a higher aspect ratio requires a larger specific power dissipation to achieve the same critical k_{La} values, power demand is rarely a significant cost factor in cells cultivation.

As a consequence other considerations, such as the larger heat transfer area available in the case of jacketed vessels, room availability, etc., might well make larger H/T ratios an interesting design option.

4. Conclusions

Oxygen transfer performance of a novel unbaffled stirred reactor has been presented in view of its use as biochemical reactor for animal cell growth. In particular, oxygen mass transfer can conveniently take place through the free vortex surface which forms when agitation speed is relatively large, yet still insufficient to inject bubbles in the liquid, so subsequent bubble bursting and related cell damage is suitably avoided. Maximum under-critical $k_L a$ values obtained ($1,7 \cdot 10^{-3} \text{ s}^{-1}$) indicate that this kind of bioreactor is fully able to satisfy the Oxygen Transfer Rate demand of typical animal cell cultures, independently of the liquid aspect ratio configuration.

Results obtained with the three configurations investigated also show that the maximum $k_L a$ achievable in sub critical conditions ($k_{La_{crit}}$) is almost independent of liquid aspect ratio. This remarkable observation implies that the expected reduction at a given agitation speed, due to slightly smaller surface area to be divided by an increasing liquid volume, is fully compensated by the further surface area and mass transfer coefficient increase due to the larger agitation velocities allowed before critical conditions are met. Despite larger aspect ratios require larger specific power demands to achieve the same $k_L a$ values, they may represent a viable option when other constraints (e.g. heat transfer requirements) make it worthwhile.

References

- Assirelli, M., Bujalski, W., Eaglesham, A., Nienow, A.W., 2008, Macro- and micromixing studies in an unbaffled vessel agitated by a Rushton turbine. *Chem. Eng. Sci.*, 63, 35-46.
- Barrett A. T., Wu A., Zhang H., Levy M. S., Lye G.J., 2010, Microwell engineering characterization for mammalian cell culture process development, *Biotechnol. Bioeng.*, 105, 260-275
- Busciglio A., Caputo G., Scargiali F., 2013, Free-surface shape in unbaffled stirred vessels: experimental study via digital image analysis, *Chemical Engineering Science*, 104, 868-880
- Chisti, Y., 2000, Animal-cell damage in sparged bioreactors. *Trends in Biotechnology*, 18, 420-432.
- Hekmat D., Hebel D., Schmid H., Weuster-Botz D., 2007, Crystallization of lysozyme: from vapor diffusion experiments to batch crystallization in agitated ml-scale vessels. *Process Biochem.*, 42, 1649–1654
- Rushton J.H., Costich E.W., Everett H.J., Power characteristics of mixing impellers - Part II, *Chem Eng Prog*, 1950, 9, 467-476
- Scargiali F., Busciglio A., Grisafi F., Brucato A., 2010a, Simplified Dynamic Pressure Method for $k_L a$ measurement in aerated bioreactors, *Biochem. Eng. J.*, 49, 165-172
- Scargiali F., Busciglio A., Grisafi F., Brucato A., 2010b, $k_L a$ Measurement in Bioreactors, *Chemical Engineering Transactions*, 20, 229-234, DOI:10.3303/CET1020039
- Scargiali F., Busciglio A., Grisafi F., Brucato A., 2012a, Oxygen transfer performance of unbaffled stirred vessels in view of their use as biochemical reactors for animal cell growth, *Chemical Engineering Transactions*, 27: 205-210, DOI: 10.3303/CET1227035
- Scargiali F., Busciglio A., Grisafi F., Brucato A., 2012b, Gas-liquid-solid Operation of a High Aspect Ratio Self-ingesting Reactor, *Int. J. Chem. React. Eng.*, 10, Issue 1, A-27, DOI: 10.1515/1542-6580.3011
- Scargiali F., Busciglio A., Grisafi F., Brucato A., 2013a, Influence of Viscosity on Mass Transfer Performance of Unbaffled Stirred Vessels, *Chemical Engineering Transactions*, 32: 1483-1488, DOI: 10.3303/CET1332248
- Scargiali F., Busciglio A., Grisafi F., Tamburini A., Micale G., Brucato A., 2013b, Power consumption in uncovered-unbaffled stirred tanks: influence of viscosity and flow regime, *Industrial & Engineering Chemistry Research*, 52, Issue 42, 14998-15005
- Scargiali F., Busciglio A., Grisafi F., Brucato A., 2014, Mass transfer and hydrodynamic characteristics of unbaffled stirred bio-reactors: influence of impeller design, *Biochemical Engineering Journal*, 82, 41- 47
- Tamburini A., Cipollina A., Micale G., Brucato A., 2012, Measurements of N_{js} and Power Requirements in Unbaffled Bioslurry Reactors, *Chemical Engineering Transactions*, 27: 343-348, DOI: 10.3303/CET1227058
- Tamburini A., Cipollina A., Micale G., Brucato A., 2013, Particle distribution in dilute solid liquid unbaffled tanks via a novel laser sheet and image analysis based technique, *Chem. Eng. Sci.*, 87, 341–358.